Chapter 1
Scientific Background

J. Jones

Abstract This chapter covers the fundamental science behind GNSS-meteorology. Firstly, atmospheric water vapour and it's role in meteorological and climate systems is covered. The Chapter then provides an overview of GNSS; how they fundamentally operate, how the atmosphere affects GNSS signals (and in particular, GNSS signal delays due to the neutral atmosphere), the conversion of atmospheric delays to integrated water vapour and the application of both signal delays and water vapour to modern meteorological observing systems.

1.1 Atmospheric Water Vapour

Water vapour is one of the most significant constituents of the atmosphere since it is the means by which moisture and energy (as latent heat) are transported through the troposphere and lower stratosphere. Aside from the role of water vapour in balancing the atmospheric heat budget, water vapour is obviously the source of precipitation. In any vertical column of air, the amount of water vapour provides operational meteorologists with a value of the maximum potential precipitation which could be retrieved from that column of air in optimal conditions. Also, as atmospheric water vapour is highly variable both temporally and spatially, it is a potential source of inaccuracy to the geodetic community, hence, accurate observations of atmospheric water vapour result in more accurate GNSS derived coordinates.

Although the actual amount of atmospheric water vapour is relatively low (~1%), the effect it has on the meteorology is very strong. It has the ability to cause temperature anomalies both large and small and, as mentioned, is also the main mechanism for atmospheric latent heat exchange. Furthermore, when looking at

Parts in this chapter are reprinted with kind permission from Jones (2010)

J. Jones (✉)
Met Office, Exeter, UK
e-mail: jonathan.jones@metoffice.gov.uk

J. Jones et al. (eds.), *Advanced GNSS Tropospheric Products for Monitoring Severe Weather Events and Climate*, https://doi.org/10.1007/978-3-030-13901-8_1

water vapour's role in the climate system, numerous scientific studies have determined that around 70% of atmospheric warming is attributable to atmospheric water vapour acting as a greenhouse gas (Houghton et al. 2001; Philipona et al. 2005).

In terms of definitions, water vapour is defined as the amount of water in gas phase (in grams per cubic metre) of air. Water vapour mixing ratio in a volume of air is the ratio of mass of water vapour and the mass of dry air. Specific humidity is the amount of water in gas phase (measured in grams in a total air volume with a mass of 1 kg). A commonly used parameter is relative humidity. Relative humidity is the ratio of the actual water vapour pressure in the air to that of the saturation (or equilibrium) water vapour pressure. Above the water vapour saturation pressure, at 100% relative humidity, any additional water vapour will condensate. The saturation pressure increases strongly with temperature, hence warm air can contain much more water vapour than cold air. Formation of clouds and precipitation is normally associated with lifting of air to levels with lower temperatures, where the air becomes over-saturated resulting in condensation.

Another way to express the water vapour content of an air parcel, is to combine all the water vapour in the vertically integrated total in any one column of air. The most commonly used terms in this case are Integrated Water Vapour (IWV) and Precipitable Water Vapour (PWV). Both terms represent the absolute total amount of water in the vertical column of air which could, hypothetically precipitate out with units of kg/m^2. The term of Integrated Water Vapour, or IWV, with units of kg/m^2 will generally be used in this report as is the standard convention in Europe. Also the unit, unlike the unit of mm which is commonly used for PWV, avoids any confusion with the units used in atmospheric delay, which are units of length. The actual amount is exactly the same, as 1 kg of water spread out over 1 m^2 would be exactly 1 mm in height.

It is important to remember that IWV is a cumulative total amount of water vapour, in principle all the way from the ground based GNSS antenna to the GNSS satellite at an altitude of around 20,000 km depending on GNSS constellation. However, water vapour is by no means distributed evenly in the vertical. The vast majority of the water vapour is limited to the warmest, bottom most portion of the lowest part of the atmosphere known as the troposphere, see Figs. 1.1 and 1.2.

In reality, the vast majority of all atmospheric water vapour is located in the bottom-most few km with a certain degree of variability depending on season, latitude and atmospheric conditions. A typical humidity profile for Camborne for July 2009 is shown in Fig. 1.2.

Due to its high variability, both temporally and spatially, water vapour is one of the most difficult quantities to predict with numerical weather prediction (NWP) models. Typically, NWP model fields are initialised using existing model data coupled with observational data. Historically, observations of water vapour were relatively scarce in meteorology with the majority of data obtained from geographically and temporally sparse radiosonde ascents. Given that approximately half of the energy in the atmosphere is transported by water vapour, other parameters such as

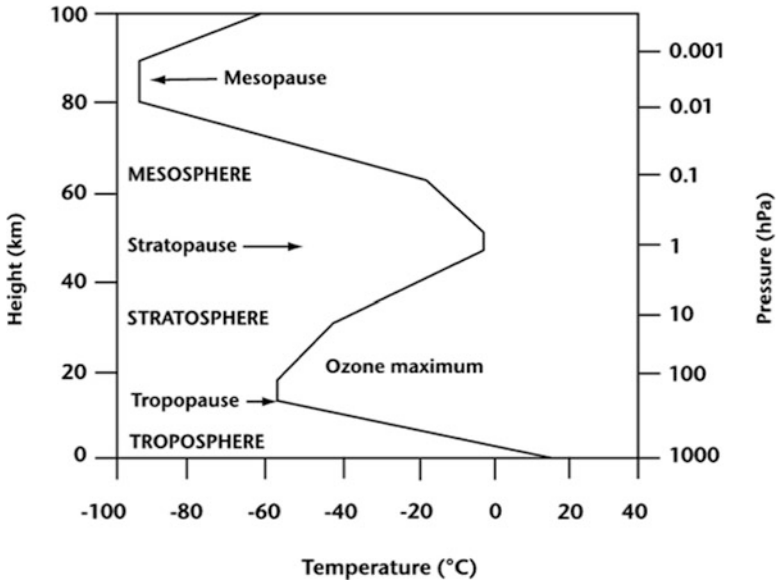

Fig. 1.1 Typical atmospheric temperature profile

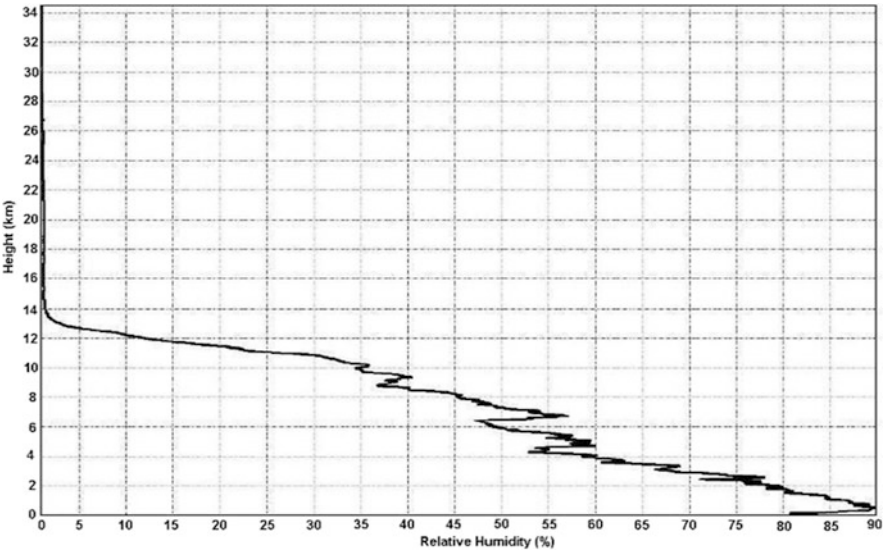

Fig. 1.2 Average monthly humidity profile, Camborne, UK. Composite of all RS92 operational radiosonde ascents from July 2009. (Courtesy of UK Met Office)

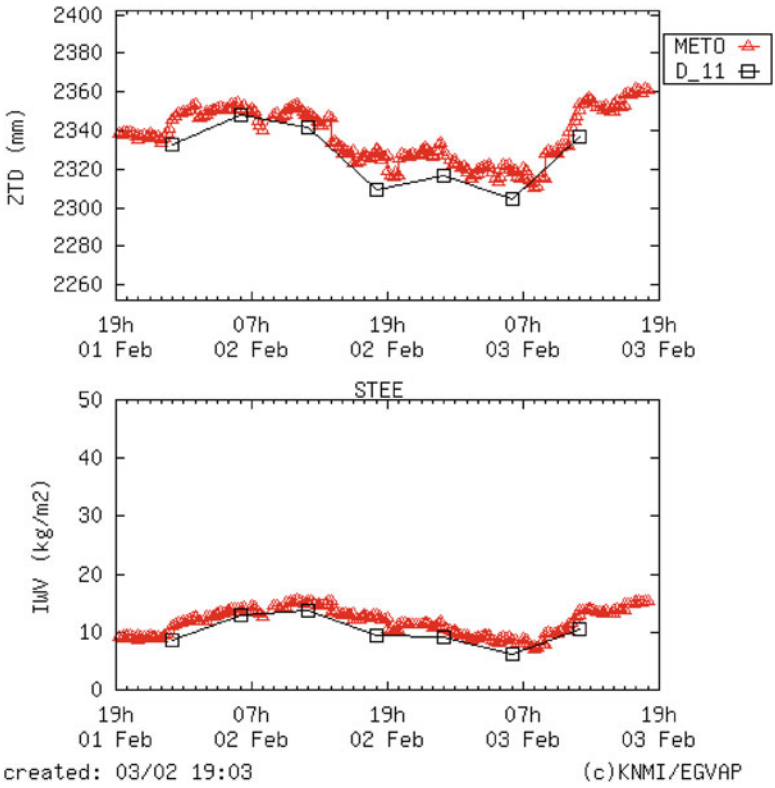

Fig. 1.3 Time series of ZTD and IWV (for Stevenage, UK, February 2010) illustrating the divergence of a NWP model which does not assimilate GNSS observations from reality

cloud cover and surface temperature are also better forecast with superior water vapour information. Due to the importance of water vapour in operational meteorology, improved knowledge and understanding of water vapour fields is one of the prime focuses for future observing systems and is key to improving future forecasting capability.

Figure 1.3 represents a time series of GPS ZTD and IWV estimates from the UK Met Office GNSS system (METO) compared against the HIRLAM 11 km unified NWP model (Unden et al. 2002) prior to the HIRLAM model assimilating GNSS ZTD observations.

In the future, added computing power will permit NWP models with ever increasing horizontal, vertical and temporal resolution. As such, with the advent of higher resolution NWP models will come the requirement for ever higher resolution observational data to initialise the models' starting conditions.

Besides the importance of accurate water vapour observations to operational meteorology, water vapour is one of the most important controlling factors in mean atmospheric temperature by the absorption of radiation. Life on Earth is very much dependent on what is commonly referred to as the greenhouse effect. In general terms, this effect is generally the absorption of solar radiation in the atmosphere, which maintains the Earth's atmosphere at a habitable temperature in which life can exist. Earth has an average temperature of around 14 °C whereas if it were not for the presence of gases such as water vapour and carbon dioxide in the atmosphere, the Earth would have a mean atmospheric temperature of around -18 °C and life would not be possible as we know it.

Water Vapour is one of the most crucial greenhouse gases and plays a vital role in the global climate system. This role is not only restricted to absorbing and radiating energy from the sun, but has direct effects on the formation of clouds and aerosols and also of the chemistry of the lower atmosphere. Despite its importance to atmospheric processes over a wide range of spatial and temporal scales, water vapour is one of the least understood and poorly described components of the Earth's atmosphere in current climate prediction models. Atmospheric water vapour allows short wavelength radiation to pass through the atmosphere, but absorbs long wavelength radiation emitted back by the Earth's surface. This trapped radiation causes the temperatures to increase.

A systematic increase in air temperature due to increasing levels of greenhouse gases, such as CO_2 and methane, enables the air to contain more water vapour. In addition, evaporation will increase where water is available (from oceans, lakes, plants, soil etc). The increase in water vapour levels leads itself to additional absorption of radiation in the lower atmosphere, but also leads to changes in the amount of cloud formation, precipitation, reflection of sunlight from cloud tops etc. Thus, water vapour is generally thought of as a feedback rather than a cause of global warming. Even so, water vapour's role in the climate system is still not very well understood. In many climate models, details in the representation of clouds can substantially affect the model estimates of cloud feedback and climate sensitivity (e.g., Senior and Mitchell 1993; Stainforth et al. 2005; Yokohata et al. 2005). Moreover, the spread of climate sensitivity estimates among current models arises primarily from inter-model differences in cloud feedbacks (Colman 2003; Soden and Held 2006; Webb et al. 2006) and as such, water vapour and it's attributable cloud feedbacks remain a large source of uncertainty in climate sensitivity estimates.

With the advent of high precision ground based geodetic GNSS networks and high quality GNSS processing schemes, we now have a novel approach for the long term monitoring of atmospheric water vapour. GNSS networks are increasing in their global coverage and if the data can be used for climate applications, they offer a huge resource in terms of monitoring atmospheric water vapour long-term. Furthermore, due to the instruments' stability, high level of reliability and low level of maintenance, GNSS sensors are especially suited to remote regions of the world which are typically data sparse. The applicability of GNSS as a tool for climate applications is discussed further in Chap. 5.

1.2 Global Navigation Satellite Systems (GNSS)

TRANSIT, was the first operational satellite navigation system. The system was developed to provide accurate location information to ballistic missile submarines. The system was rolled out for military use in January 1964 and subsequently to civilian users in July 1967. The system, using a constellation of five polar orbiting satellites in low Earth orbit (1075 km) was comprised of two carrier frequencies (150 and 400 MHz) which could be used to provide an hourly positioning estimate with an accuracy of between 200 and 400 m.

However, it wasn't until 1993 when the Global Positioning System (GPS) achieved operational capability that continuous three dimensional positioning and timing information became widely available allowing positioning accuracy down to the sub-decimetre level. The basic principle of GPS is that coded signals are transmitted by at least four satellites for the three dimensional position, plus the time element, to be determined. More information on the technique is given in the subsection below focusing on GPS basics. Whilst other GNSS systems are of course available and operational, the focus here is on GPS only - all other GNSS systems use the same basic principles (Fig. 1.4).

1.2.1 GPS Basics

All GNSS consist of three primary segments: space, ground and user. The space segment consists of satellites orbiting at an altitude of (in the case of GPS) approximately 20,200 km in orbital planes of 55 degrees to the equator. There must be at least 24 satellites operational to ensure at least 4 satellites are visible at any point on the Earth's surface, at any one time. The satellites transmit coded signals and other information (orbital parameters, satellite clock errors etc.) to the user. The ground segment consists of a master control station (in Colorado, USA for the GPS), as well

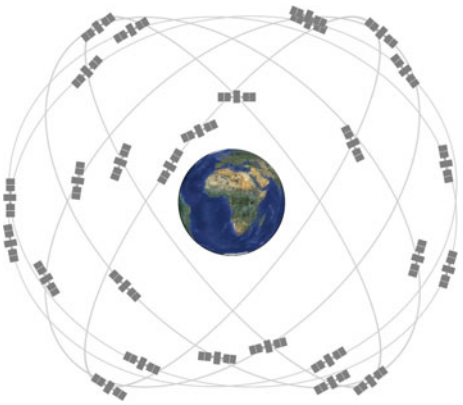

Fig. 1.4 Representation of a GNSS satellite constellation

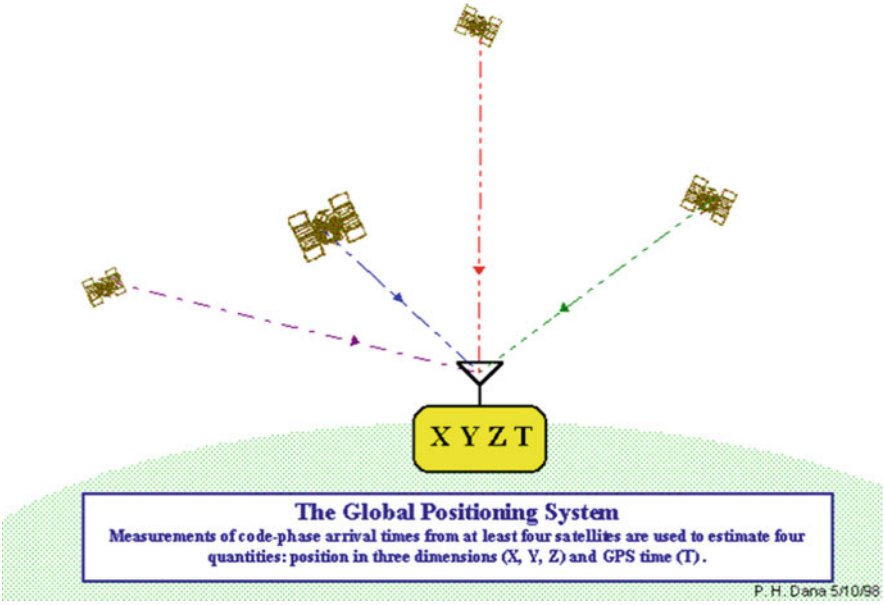

Fig. 1.5 Illustration of GPS positioning

as a number of global monitoring stations, which are responsible for estimating essential satellite information such as orbits and clock errors.

On each GPS satellite, an onboard satellite oscillator generates the fundamental frequency (f_0) of 10.23 MHz from which all other GPS signals are derived. Until relatively recently only two GPS sinusoidal carrier frequencies f_1 and f_2 (at 1575.42 MHz and 1227.60 MHz respectively) were generated which are right-hand polarized with respect to each other and are modulated with coded information. There are three codes imposed on the signal, the C/A (Coarse Acquisition or Clear-Access) code, the P (Precise or Protected) code and the navigation message. These codes have two states, a + 1 or −1 state. As such if the phase-modulated L1 and L2 codes can be decoded by a ground based GPS receiver (the user segment) they may give the user positioning and velocity information, as summarised in Fig. 1.5. In recent times, additional GPS frequencies are transmitted such as L5 and L2C, however, the fundementals of how the system is operated and it's application to meteorology is still largely based around the original two GPS frequencies.

The C/A code has a code sequence of 1023 bits in length and is transmitted with a frequency of 1.023 MHz. As such, it repeats itself once every millisecond and assuming the signal is travelling at the speed of light the distance between subsequent chips can be estimated to be ~300 m. The generation of the P-Code is very similar with the length of the code sequence being approximately 2.3547×1014 bits which corresponds to a time span of approximately 266 days. The P-Code repeats itself once every week and through a process known as anti-spoofing (AS), the P-code is encrypted to a Y-code.

After signals are received by a GPS receiver, the signals are initially split into their satellite specific pseudorandom noise or PRN number based on the C/A codes. A carrier reference code is generated by the GPS receiver, modulated with a copy of the satellite specific PRN code and time shifted to compare against the received code. If the receiver and satellite clock errors are ignored, this difference gives the travel time (τ) and when multiplied by the speed of light (c) gives the approximate range or pseudo-range to the satellite.

Phase positioning measurements are based on reconstructing the carrier phase of the signal and comparing against a signal copy generated by the GPS receiver. By observing the difference in the phase of the signals transmitted by the GPS satellite and those stored in the GPS receiver, the phase difference may be obtained which can be resolved to provide the user with a distance measurement. This expression may be written as:

$$\Delta\phi = \phi_{obs} - \phi_{rec} \tag{1.1}$$

Positioning using phase differencing has a much higher accuracy, although it does introduce an integer ambiguity (j_{amb}) which must be solved for. Furthermore additional delays in the signal propagation such as ionospheric delay (ΔL_{ion}), tropospheric delay (ΔL_{trp}) and clock differences between the satellite and receiver ($\tau_{sat} - \tau_{rec}$) must all be accounted for if precise, geodetic positioning is to be achieved. From Blewitt (1997) the pseudorange, multiplied by the frequency, λ, may be expressed as:

$$\lambda\Delta\phi = D + c(\tau_{sat} - \tau_{rec}) - \lambda j_{amb} + \Delta L_{trp} + \Delta L_{ion} + \mathrm{E} \tag{1.2}$$

Where D is the geometric range from receiver to satellite, c is the speed of light and E is the unknown errors such as receiver multipath. As there are more unknown parameters in Eq. 1.2 than known parameters, equations for a number of satellites are required if all parameters are to be solved for. Furthermore, satellite orbit and clock information must be known a-priori which can be obtained from the International GNSS Service (IGS), which is a voluntary federation of more than 200 worldwide organisations generating and providing free-of-charge GNSS products and services. With particular reference to this report, the IGS are essential in providing satellite clock corrections as well as both predicted and past satellite orbit information.

Even though the clock files provided by the IGS are of high quality there still remain clock errors in both satellite and receiver as well as un-calibrated phase errors which must be accounted for. These errors are common to all receivers and satellites and they can be eliminated by observing a number of satellites and receivers and forming what are known as baselines. Single difference baselines are formed by observing the same satellite by two receivers, in this way the satellite clocks and phase errors can be eliminated. By observing two satellites by two receivers the satellite clock, receiver clock and phase errors are all eliminated. However,

tropospheric errors can only be ignored if the baselines are relatively small and the stations are at roughly the same altitude, as the effect from the atmosphere will affect all signals in the same way.

The alternative to forming baselines between receivers to remove the clock errors, is to resolve the clock errors a-priori and thus introduce very accurate clock files into the processing in the first place. If this can be achieved, a network of GPS receivers can be processed in a station specific way, which is commonly referred to as Precise Point Positioning or PPP. The main benefits of PPP are that it is, at least for the coordinate and tropospheric estimation part, faster because the sites can be processed individually and the processing load can be shared over a number of CPUs/servers. Also, as the sites are processed individually, there is no risk of correlated errors as could be the case with the network solution. In reality however, any benefits in processing speed are often offset against the time it takes to generate the higher accuracy clocks and as such, the overall processing time for a national scale (approximately 200-receiver) network is often comparable to that taken by a double difference (DD) solution. It is when processing larger GNSS networks (300+ stations) where PPP typically has a speed advantage over DD. Furthermore, while a PPP system might not have any correlated errors between different parts of the network due to baselines, if any errors are introduced in the satellite clock determination part, those errors will be applied to the whole network being processed. For more information on the PPP method, see Kouba and Heroux (2001).

1.2.2 Delay in the Neutral Atmosphere

Once enough data has been collected from a number of satellites over a long enough time period, estimates can be generated of atmospheric delay as well as satellite clock errors and phase ambiguities. Due to the dispersive nature of the ionosphere it affects both GPS signals in the same way, by a mathematical combination of the L1 and L2 signals, a so-called ionosphere-free linear combination (L3) can be obtained and thus first order ionospheric delays can be eliminated. Second order effects are still present but their order of magnitude is so small they can be largely ignored for the purposes of this report.

$$L_3 = \frac{f_1^2}{f_1^2 - f_2^2} L_1 - \frac{f_2^2}{f_1^2 - f_2^2} L_2 \tag{1.3}$$

The atmosphere local to the GPS receiver is typically assumed to be horizontally homogenous and based on this assumption, slant path delays can be mapped into the vertical and the number of unknowns can be reduced further. While there is not enough power in the least squares adjustment to solve for slant paths directly, slant path delays are research topics at a number of atmospheric and geodetic institutes, but use of a-priori atmospheric model information is often necessary (Fig. 1.6). More

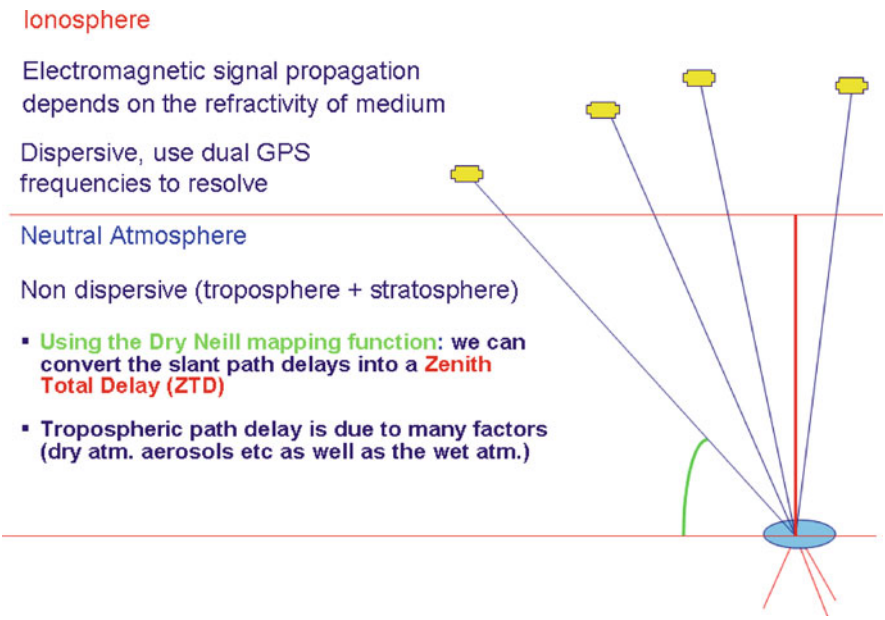

Fig. 1.6 Schematic of satellite signal path through atmosphere

information on slant delays and tomographic retrieval can be found in Chap. 3 of this report.

Tropospheric delay can be expressed as:

$$\Delta^T = \int_s n ds - \int_g dg \tag{1.4}$$

where n is the refractive index, s is the actual signal path and g is the hypothetical geometric path. It is possible to rewrite this as:

$$\Delta^T = \int_s (n-1) ds + \left(\int_s ds - \int_g dg \right) \tag{1.5}$$

This expression shows us that tropospheric delay is a combination of the excess geometric path length as well as the slowing of the signal propagation speed.

Excess geometric path length caused by changes in refractive index, n, is only of relevance at very high zenith angles where the signal is effectively being bent by the atmosphere and a bending angle is introduced. At the vast majority of satellite zenith angles, bending and thus excess path length is very small when compared to the delay of the signal due to propagation. From McClatchey et al. (1971) geometric delay at a zenith angle of 80° would only be in the region of ~4 cm whereas at lower zenith angles (i.e. higher elevation angles) the delay due to slowing of the signal contributes to around 99.7% of the atmospheric delay. In current practice, most GPS

receivers are set with an elevation cut off angles of either 5° or 10° which largely eliminates the geometric delay, as well as minimizing the multipath effect of signals being reflected off the Earth's surface or nearby objects.

As such we can we-write Eq. 1.5 to show that the tropospheric delay is due to the integrated refractivity along the signal propagation path:

$$\Delta^T = \int_s (n-1)ds = 10^{-6} \int_s Nds \tag{1.6}$$

where refractivity N is defined as $N = 10^6 (n-1)$ (according to Smith and Weintraub 1953; Thompson et al. 1986). In the microwave range however refractivity is related to atmospheric parameters through:

$$N = k_1 \frac{p_d}{T} Z_d^{-1} + k_2 \frac{e}{T} Z_w^{-1} + k3 \frac{e}{T^2} Z_w^{-1} \tag{1.7}$$

Where p_d is the pressure of dry air, e is the water vapour pressure, T is the temperature, Z_d and Z_w are the compressibility factors of dry air and water vapour respectively and k_1, k_2 and k_3 are thermodynamic coefficients with values of 77.6 $KhPa^{-1}$, 70.4 $KhPa^{-1}$ and 373,900 K^2 hPa^{-1} respectively, taken from Thayer (1974).

1.2.3 Zenith Delay Estimates

One of the standard outputs from a number of geodetic GNSS processing software is the Zenith Total Delay or ZTD, based on phase measurements from a network of ground based receivers. In GNSS-meteorology it is useful to reduce the term of ZTD into its constituent parts; Zenith Hydrostatic Delay (ZHD) and Zenith Wet Delay (ZWD). ZHD is responsible for the vast majority of the ZTD delay (typically around 90%) but is easily modeled if atmospheric pressure is known. It is the ZWD, which is of particular interest to meteorology, as it is this component which is related to humidity and can change rapidly both spatially and temporally. If we assume that the dry and wet components of Eq. 1.7 behave as ideal gases, Z_d and Z_w are equal to 1 (Bevis et al. 1992) and can therefore be eliminated. Such that when we separate the pressure into its dry and wet partial pressures we can express these terms as:

$$\rho_d = \frac{p_d}{R_d T} \tag{1.8}$$

and

$$\rho_w = \frac{e}{R_w T} \tag{1.9}$$

where R_d and R_w are the gas constants of dry air and water vapour respectively. The density of the 'real' air is simply $\rho_d + \rho_w$. Therefore the refractivity can be expressed as:

$$N = k_1 \frac{p_d}{T} + k_2 \frac{e}{T} + k3 \frac{e}{T^2} \tag{1.10}$$

which can be further reduced to:

$$N = k_1 \rho R_d + (k_2 R_w - k_1 R_d)\rho_w + \frac{k_3 \rho_w R_w}{T} \tag{1.11}$$

Since the path is assumed to be zenithal, ZTD is equal to Δ^T and therefore we can integrate Eq. 1.6, so that ZTD between the receiver altitude z_r and infinity is:

$$ZTD = 10^{-6} \int_{z_r}^{\infty} N dz \tag{1.12}$$

And therefore:

$$ZTD = 10^{-6} \int_{z_r}^{\infty} k_1 \rho R_d dz + 10^{-6} \int_{z_r}^{\infty} (k_2 R_w - k_1 R_d)\rho_w dz + 10^{-6} \int_{z_r}^{\infty} \frac{k_3 \rho_w R_w}{T} dz \tag{1.13}$$

1.2.4 Derivation of IWV from ZTD

The first term on the right hand side of Eq. 1.13 deals with the integration of the combined wet and dry air, The second and third terms integrate the water vapour density and ratio of water vapour density and temperature respectively. Furthermore by application of the hydrostatic equation:

$$dp = -g\rho dz \tag{1.14}$$

where g is the local gravitational acceleration, allows us to transform the first term of Eq. 1.13 to:

$$ZHD = 10^{-6}\frac{k_1 R_d}{g^*}p_r \tag{1.15}$$

where $g^*$is the local gravitational acceleration and the centre of mass of the vertical air column and the integration is performed between 0 and pressure at the receiver p_r. Equation 1.15 shows the dependency between receiver pressure and ZHD. However, as is illustrated in Eq. 1.13, other atmospheric parameters need to be known (temperature, humidity etc.) to determine the wet component of the delay. As this information is not necessarily available certain assumptions about the state of the atmosphere must be made.

By making additional assumptions about the vertical temperature and humidity structure, we can transform ZWD into a more meteorological term, integrated water vapour (IWV):

$$\mathrm{IWV} = \int_{z_r}^{\infty} \rho_w dz \tag{1.16}$$

So,

$$\begin{aligned}\mathrm{ZWD} &= 10^{-6}\int_{z_r}^{\infty}(k_2 R_w - k_1 R_d)\rho_w dz + 10^{-6}\int_{z_r}^{\infty}\frac{k_3 \rho_w R_w}{T}dz \\ &= 10^{-6}\left((k_2 R_w - k_1 R_d)\int_{z_r}^{\infty}\rho_w dz + 10^{-6}k_3 R_w \int_{z_r}^{\infty}\frac{\rho_w}{T}dz\right.\end{aligned} \tag{1.17}$$

To derive a relationship between ZWD and IWV we must first derive a mean temperature the vertical column of air above the GPS receiver

$$T_m = \frac{\int_{z_r}^{\infty}\rho_w dz}{\int_{z_r}^{\infty}(\rho_w/T)dz} \tag{1.18}$$

And as this relation is identical to

$$\int_{z_r}^{\infty}\frac{\rho_w}{T}dz = \frac{\int_{Z_r}^{\infty}\rho_w dz}{T_m} \tag{1.19}$$

The ZWD Eq. 1.17 can now be rewritten as

$$ZWD = 10^{-6}\left(k_2 R_w - k_1 R_d + k_3\frac{R_w}{T_m}\right)\int_{z_r}^{\infty}\rho_w dz \tag{1.20}$$

$$ZWD = 10^{-6}\left(k_2 R_w - k_1 R_d + k_3\frac{R_w}{T_m}\right)IWV \tag{1.21}$$

The conversion of ZTD into IWV thus depends largely on the mean temperature of the air column (T_m), which in turn depends on the vertical temperature and humidity profiles. The estimation of vertical temperature and humidity introduces error into the ZWD to IWV conversion and for this reason ZTD is more commonly assimilated into NWP assimilation schemes as opposed to IWV.

References

Bevis, M., Businger, S., Herring, T. A., Rocken, C., Anthes, R. A., & Ware, R. H. (1992). GPS meteorology: Sensing of atmospheric water vapor using the global positioning system. *Journal of Geophysical Research, 97*, 15787–15801.

Blewitt, G. (1997). Basics of the GPS technique: observation equations. In B. Jonsson (Ed.), *Geodetic applications of GPS* (pp. 9–54). Helsinki: National Land Survey of Sweden.

Colman, R. (2003). A comparison of climate feedbacks in general circulation models. *Climate Dynamics, 20*, 865–873.

Houghton, J. T., Ding, Y., Griggs, D. J., Noguer, M., van der Linden, P. J., Dai, X., Maskell, K., & Johnson, C. A. (Eds.). (2001). *Climate change 2001: The scientific basis*. Contribution of Working Group I to the third assessment report of the Intergovernmental Panel on Climate Change. Cambridge, UK: Cambridge University Press.

Jones, J. (2010). *An assessment of the quality of GPS water vapour estimates and their use in operational meteorology and climate monitoring*. PhD thesis, University of Nottingham. http://eprints.nottingham.ac.uk/11287/1/JJ_Thesis_Final.pdf

Kouba, J., & Heroux, P. (2001). Precise point positioning using IGS orbit and clock products. *GPS Solutions, 5*(2), 12–28.

McClatchey, R. A., Fenn, R. W., Selby, J. E. A., Volz, F. E., & Garing, J. S. (1971). *Optical properties of the atmosphere* (p. 85). Report AFRCL-71-0279. Air Force Cambridge Research Laboratories.

Philipona, R., Dürr, B., Ohmura, A., & Ruckstuhl, C. (2005). Anthropogenic greenhouse forcing and strong water vapour feedback increase temperature in Europe. *Geophysical Research Letters, 32*, L19809. https://doi.org/10.1029/2005GL023624.

Senior, C., & Mitchell, J. (1993). Carbon dioxide and climate. The impact of cloud parameterization. *Journal of Climate, 6*, 393–418.

Smith, E. K., & Weintraub, S. (1953). The constants in the equation for atmospheric refractive index at radio frequencies. *Proceedings of the IRE, 41*, 1035–1037.

Soden, B. J., & Held, I. M. (2006). An assessment of climate feedbacks in coupled ocean-atmosphere models. *Journal of Climate, 19*, 3354–3360.

Stainforth, D. A., Aina, T., Christensen, C., Collins, M., Faull, N., Frame, D. J., Kettleborough, J. A., Knight, S., Martin, A., Murphy, J. M., Piani, C., Sexton, D., Smith, L. A., Spicer, R. A., Thorpe, A. J., & Allen, M. R. (2005). Uncertainty in predictions of the climate response to rising levels of greenhouse gases. *Nature, 433*(403), 406.

Thayer, G. D. (1974). An improved equation for the radio refractive index of air. *Radio Science, 9*, 803–807.

Thompson, A. R., Moran, J. M., & Swenson, G. W. (1986). *Interferometry and synthesis in radio astronomy* (720pp.). New York: Wiley.

Unden, P., Rontu, L., Jarvinen, H., Lynch, P., Calvo, J., Cats, G., Cuhart, J., & Eerola, K. (2002). *HIRLAM-5 scientific documentation*. Technical report, HIRLAM-project, Norrkopping.

Webb, M. J., Senior, C., Sexton, D., Ingram, W., Williams, K., Ringer, M., Mcavaney, B., Colman, R., Soden, B., Gudgel, R., Knutston, T., Emori, S., Ogura, T., Tsushima, Y., Andronova, N., Li, B., Bony, S., & Taylor, K. (2006). On the contribution of local feedback mechanisms to the range of climate sensitivity in two GCM ensembles. *Climate Dynamics, 27*, 17–38.

Yokohata, T., Emori, S., Nozawa, T., Tsushima, Y., Ogura, T., & Kimoto, M. (2005). A simple scheme for climate feedback analysis. *Geophysical Research Letters, 32*, L19703. https://doi.org/10.1029/2005GL023673.